2020 IEEE/RSJ International Conference on Intelligent Robots and Systems (IROS)
October 25-29, 2020, Las Vegas, NV, USA (Virtual)

Tracking Strategy Based on Magnetic Sensors for Microrobot Navigation in the Cochlea

Tarik Kroubi[1] Karim Belharet[2] and Kamal Bennamane[1]

Abstract— **One approach to control drug delivery in the cochlea is to use a magnetic microrobot powered by externally applied magnetic fields. However, it is necessary to integrate a localization system to ensure the precise navigation of the microrobot in the cochlear canal. To avoid integrating a clinical imaging modality for the navigation of microrobots in the cochlea, we propose in this work the application of magnetic sensors to localize the magnetic microrobot. In our method, we propose a real-time localization system based only on two sensors to keep a precise localization of the spherical magnetic microrobot. The first sensor measures both the magnetic field of the environment and the magnetic field generated by the microrobot (localization sensor). The second sensor (surrounding sensor) is placed away from the localization sensor, this sensor measures the magnetic field of the environment, which will be subtracted from the signal of the localization sensor to determine the value of the magnetic field of the microrobot. We have proposed a new magnetic sensor calibration method and a robust localization algorithm for precise localization of the microrobot. The experiments demonstrate the effectiveness of the designed system and show the precision of the proposed localization strategy.**

Index Terms— **Magnetic microrobot, magnetic field, magnetic sensor, localization**

I. INTRODUCTION

The administration of cochlear drugs has gradually shifted from systemic administration to local administration for several reasons. The systemic route of administration of the drug is limited due to the blood-cochlear barrier which prevents the diffusion of blood in the cochlea [1] [2], and requires increasing the doses of administration of drugs by oral or intravenous route [3], which considerably limits the number of candidate drugs and duration of treatment. In addition, the need for long-term treatment and significant undesirable side effects further limit the use of systemic administration [4], [5]. Among the suggested local methods of local drug delivery to the inner ear, a minimally invasive method has been used for several years in clinical practice. This method involves injecting the drug into the middle ear through the tympanic membrane under local anesthesia. In this way, the drug is in contact with the round window membrane (RWM), and thanks to the RWM structure and its permeability characteristics, the drug diffuses inside the cochlea [6]. However, the amount of medication delivered to the inner ear is poorly controlled by this method [7]. In addition, the diffusion inside the cochlea beyond the basal turn is very limited because the peril-lymphatic flow is very low [8].

One approach to controlled drug delivery to the cochlea is to use magnetic microrobot actuated with externally applied magnetic fields. We previously studied the navigation of a magnetic microrobot inside the cochlea using a magnetic actuator composed of two permanent magnets [9] [10]. In another work, we have proposed a four-permanent-magnets-based actuator, to steer magnetic micro-robots in the cochlea [11]. This actuator offers the appreciable ability to both push and pull microrobots, unlike single-permanent-magnet that offers only pulling forces. We even have evaluated the feasibility of superparamagnetic nanoparticles (SPMNP) delivery to the apex, and to assess the hearing function in the presence of intracochlear SPMNP [12].

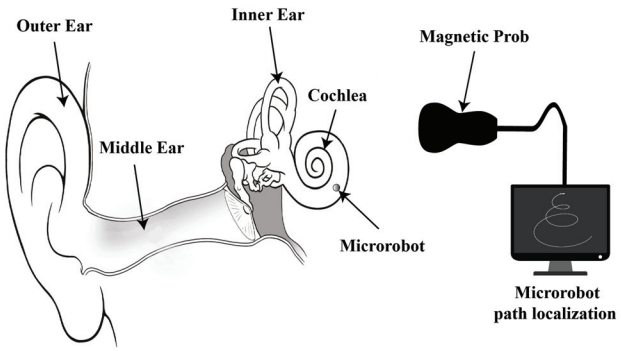

Fig. 1. Overview of the three-dimensional localization of a magnetic microrobot navigating in the human inner ear (cochlea).

However, it is indispensable to integrate a clinical imaging modality for microrobot navigation in a human-sized medical application [13]. One of the alternatives for using magnetic actuation systems without medical imaging modality consists of using magnetic sensors to detect and localize microrobots in the human body. Indeed, various localization methods using magnetic sensors are proposed by several groups [14]–[18]. Most of these systems are developed for the detection and localization of an endoscopic capsule. Indeed, due to the

This work was supported by Franco-Algerian overseas scholarship PROFAS B+ and the CochléRob project funded by HEI campus Centre, Châteauroux Métropole and Région Centre.

[1] Tarik kroubi is with Hautes Études d'Ingénieur campus Centre, PRISME, Châteauroux, France and Department of Electronics, University of Mouloud Mammeri, Tizi-Ouzou 15000, Algeria tarik.kroubi@yncrea.fr

[1] Kamal Bennamane is with the Department of Electronics, University of Mouloud Mammeri, Tizi-Ouzou 15000, Algeria kabennamaneg@gmail.com

[2]Karim Belharet is with Hautes Études d'Ingénieur campus Centre, PRISME EA 4229, Châteauroux, France karim.belharet@yncrea.fr

technological limitation of magnetic sensors, the problem of detecting magnetic microrobots dedicated to the administration of drugs in the human body has never been studied. However, for some applications such as non-deep organs of the human body, the sensors are able to detect a magnetic microrobot.

In this paper, we demonstrate the ability to localize magnetic microrobot injected in the cochlea (Fig.1). A key strategy is to use magnetic sensors to detect a magnetic field generated by the microrobot. Section II introduces the proposed methodology for localizing a microrobot using magnetic sensors. Section III describes the experimental bench developed to validate the proposed localization methodology as well as the associated experimental results. This paper is concluded in Section IV.

II. METHODOLOGY

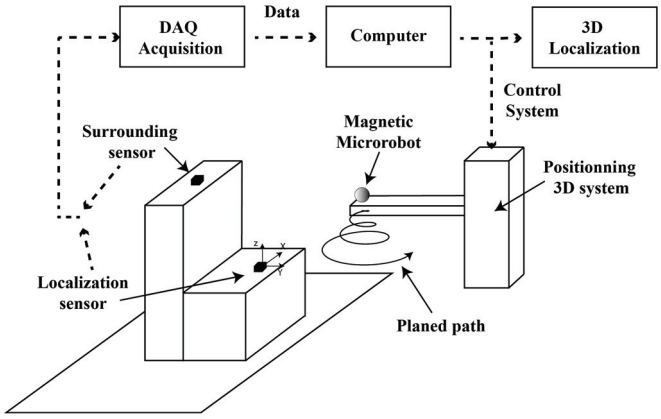

Fig. 2. Global architecture of the localization system.

In our method, we propose the real-time localization system based only on two sensors for the localization of a magnetic microrobot with accuracy. As shown in Fig.2, the operating principle consists in calculating the 3D position of a magnetic microrobot mounted on a micrometric three axial positioning system. The latter can reach an accuracy of 1 μm, which is enough to validate the accuracy of our system. The micrometric three axial positioning system on which the magnetic microrobot is mounted is used to execute a planned trajectory via the computer using Matlab and Labview software. The movement of the magnetic microrobot is tracked by the localization system and displayed on the screen. The localization system is composed of two identical magnetic sensors designed by Honeywell for a weak magnetic field. The first sensor is used for the localization of the magnetic microrobot (localization sensor). The second (Surrounding sensor) positioned away from the localization sensor, that aim to measure the magnetic field of the environment (Earth's geomagnetic field and nearby ferromagnetic) and subtract it from the localization sensor's signal (Fig.3).

This subtraction step only detects the magnetic field of the magnetic microrobot and calculates its position using the

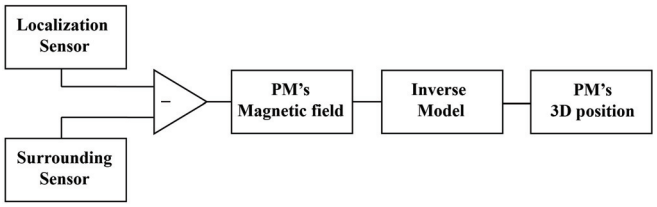

Fig. 3. Surrounding magnetic field Subtraction step

reverse dipole model as shown in the diagram of the Fig.3. Two conditions are essential for a successful subtraction:

- First, the two sensors must be rigidly linked, aligned in the same direction.
- Second, the two sensors must be calibrated simultaneously.

This method allows us not only to remove a noisy magnetic field but also to make the localization system insensitive to possible movements of the sensors, since the origin of the coordinate system is the center of the localization sensor itself. That was validated by an experimental setup that we will see later in the experimental section.

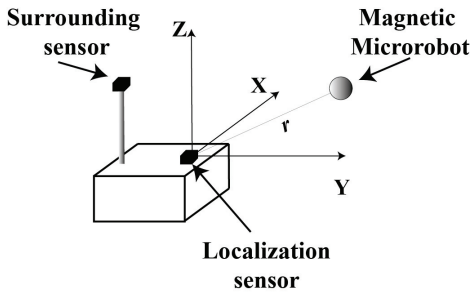

Fig. 4. Localization sensor's coordinate system

A. Magnetic field model of magnetic microrobot

The magnetic dipole model is generally used to model a permanent magnetic source [19] [20] [21]. Its magnetic flux density measured by the magnetic sensor can be expressed as [22], [23]:

$$\vec{B} = \frac{\mu_0}{4\pi} \overrightarrow{grad} \left[\frac{\vec{m} \cdot \vec{r}}{r^3} \right] \tag{1}$$

Solving the equation (1) yields the model of the magnetic flux density in three dimension as follow:

$$\vec{B} = \frac{\mu_0}{4\pi} \left[\frac{3(m.r)r}{r^5} - \frac{m}{r^3} \right] \tag{2}$$

Where:

- $\mu_0 = 4\pi * 10^{-7} H/m$, is the magnetic air permeability.
- $m = M * V$ is the magnetic dipole moment where the magnetization $M = 1.05 * 10^6 A/m$, and V is the magnetic microrobot volume
- r is the position vector $[x, y, z]^T$ of a magnetic microrobot

The magnetic microrobot used for the simulation is N42 grade, nickel plated neodymium-iron-boron (NdFeB) rare earth magnet. The remnant magnetic flux density is $Br = 1,32T$ (N42), which correspond to internal magnetization $M = \frac{B_r}{\mu_0} = 1,05 * 10^6 A/m$ and radius $a = 1,5mm$. These parameters were initially simulated under Comsol Multiphysics to illustrate the intensity of the magnetic field (B), generated by the magnetic microrobot and its components (B_x, B_y, B_z) in a 3D workspace. The (Fig.5-a) shows the simulation results using Comsol Multiphysics software. We also simulated the analytical model that will be exploited in the localization algorithm. The comparison results between the numerical model (Comsol) and the analytic model (Matlab) are illustrated in the figures (Fig.5-b), (Fig.5-c) and (Fig.5-d). The simulations results show that the analytical model is in good correlation with the numerical model. We can, therefore, trust this analytical model, and use it to localize the magnetic microrobot from the measured magnetic field.

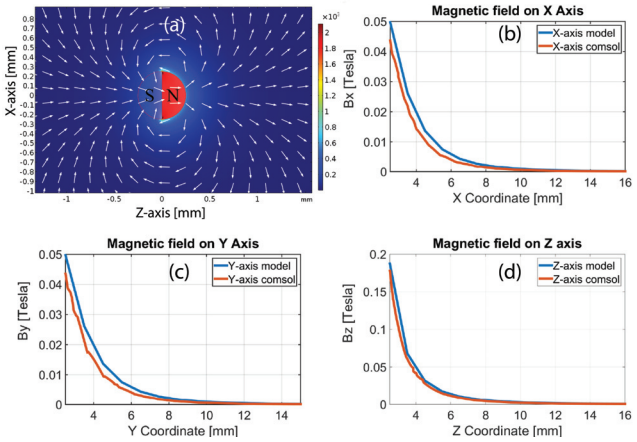

Fig. 5. Magnetic field simulation produced by the magnetic microrobot. (a) is the Comsol simulation in three dimension, (b),(c),(d) are the three magnetic filed components b_x, b_y, b_z comparison under Matlab (analytic model) and Comsol (numerical model)

B. Magnetic sensor calibration

The accuracy of the magnetic tracking system depends entirely on the magnetic sensor output. In fact, the vector position of the magnetic microrobot is in close relation with its generated magnetic field. This is what links the position of the magnet to its magnetic field. Thereby, any modification of the magnetic sensor output data like Earth's magnetic field, nearby ferromagnetic (soft and hard iron), misalignment of the sensor with the fixed coordinate system, sampling noise, sensitivity mismatch and offset drifts, cause errors on the localization of the magnetic microrobot. Calibrating the magnetic sensors before the vector position is more then primary. In the state of the art, generally, this step is neglected and is compensated by increasing the number of sensors to reduce localization errors. Some research does partial calibration to compensate for systematic and misalignment errors, which is insufficient to develop an accurate magnetic tracking system.

The unwanted magnetic fields can be classified into two distinct groups, hard and soft iron errors. The basic idea of calibration in the magnetic field domain is that the locus of the error-free measurements of a 3D magnetometer is a sphere, its as shown in the following expression:

$$(h_x)^2 + (h_y)^2 + (h_z)^2 = h^2 \tag{3}$$

where: h_x, h_y, h_z are three-axis x, y, z of the magnetometer respectively and h is the magnitude of the local earth magnetic field vector which is a function of geographical location. The effect of the various magnetometer errors is to alter the shape of the locus described by the equation (3), this erroneous magnetometer outputs is noted $\hat{h}(\hat{h_x}, \hat{h_y}, \hat{h_z})$. The equation for the locus of the magnetometer measurements becomes:

$$\left(\frac{\hat{h_x} - b_x}{\alpha}\right)^2 + \left(\frac{\hat{h_y} - b_y}{\beta}\right)^2 + \left(\frac{\hat{h_z} - b_z}{\gamma}\right)^2 = h^2 \tag{4}$$

The equation (4) is an ellipsoid equation with (b_x, b_y, b_z) center and (α, β, γ) radius. The conic form of an ellipsoid (5) is defined with 9 parameters. These parameters are: three coordinates of the center (X_0, Y_0, Z_0), three radius (a, b, c) and three rotational angles (θ, ψ, ω) which represent rotations around x, y and z axis respectively [24].

$$\begin{aligned} &Ax^2 + By^2 + Cz^2 + 2Dxy + 2Exz + 2Fyz + \\ &2Gx + 2Hy + 2Iz - 1 = 0 \end{aligned} \tag{5}$$

where: (x, y, z) are data collected from magnetometer triad $(\hat{h_x}, \hat{h_y}, \hat{h_z})$ above. The algebraic form is as follow:

$$v^T \hat{A} v = 0$$

where:

$$\hat{A} = \begin{bmatrix} A & D & E & G \\ D & B & F & H \\ E & F & C & I \\ G & H & I & -1 \end{bmatrix}, \; v = [x \; y \; z \; 1]^T$$

The final calibrated data are as follows:

$$[\hat{h_x}^c, \hat{h_y}^c, \hat{h_z}^c]^T = M_T * \left([\hat{h_x}, \hat{h_y}, \hat{h_z}]^T - [a, \; c, \; d]^T\right) \tag{6}$$

with, M_T the transformation matrix.

According to the equation (6), to perform the calibration procedure, we need to make magnetic field measurements with the sensor. It is important to take measurements in different positions and in all directions. For this, we have developed a measuring bench dedicated to the calibration of the magnetic sensors (Fig.6).

To calibrate the sensor, we must first rotate the magnetic sensors (both sensors) in all directions using a calibration bench developed for this purpose (Fig.6) around the

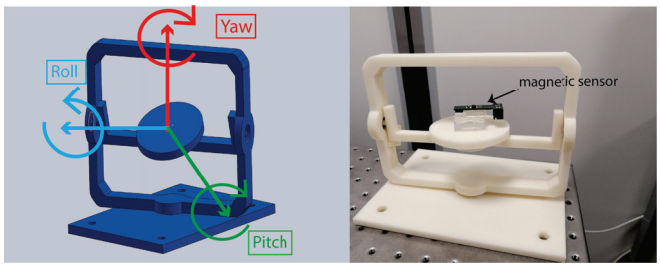

Fig. 6. Calibration setup: (a) CAD model, (b) 3D printer prototype.

workspace without the presence of magnetic microrobot. The measured magnetic field at different positions and orientations is recorded. Then, these measurements are used with the calibration algorithm presented above to calculate the calibration parameters. The results of the calibration step are presented in (Fig.7). The first step is the ellipsoid fit to the raw measurement data set, that provides the calibration parameters of the sensors (see Fig.7-a). (Fig.7-b) shows all the measurement data of the magnetic sensor before (red) and after calibration (blue).

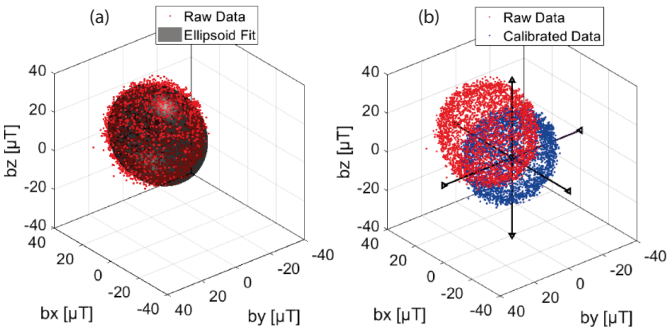

Fig. 7. (a) Ellipsoid fit to raw data, (b) data after the calibration step.

Most of the work found in the literature neglects this calibration step and opt instead on increasing the numbers of magnetic sensors to decrease localization errors, but as shown in (Table 1), if we place the magnetic microrobot on the same distance (measured before) in the positive direction then in the negative direction of one of the uncalibrated magnetic sensor axes, the corresponding absolute value of the measured magnetic field is different, which results in errors in the calculation of the position vector.

Table I shows the measurement results of the magnetic field in both positive and negative directions of each axis of the magnetic sensor, before and after calibration. As we can see in the table, important error between the magnetic field measured in the two directions of each axis of the three components Bx, By and Bz of the magnetic sensor. However, this error is significantly reduced after the calibration procedure.

C. Localization algorithm

The magnetic field model generated by a magnetic microrobot has been introduced in the equation (2). Due to the strong non-linear relationship between the intensity of the magnetic field and the position of the magnetic microrobot, this model is difficult to reverse. For this, an appropriate nonlinear optimization algorithm must be used to solve this equation. Several optimization methods have been proposed in the literature [25] . The Levenberg-Marquardt (L-M) algorithm was selected because it is faster (< 0.11 seconds in Matlab) and more accurate than others. The objective function is defined as follows:

$$E = \sum_{i=1}^{N} (B^i_{meas} - B^i_{calc})^2 \tag{7}$$

where B_{meas} are the calibrated data and measured with the localization sensor, and the B_{calc} is the function of the position parameters (x, y, z). The L-M algorithm is called Nonlinear Least Squares Minimization [26], it aims to vary (x, y, z) to minimize E and get the solution of the function.

The L-M algorithm is used to calculate the three-dimensional position vector $[x, y, z]^T$ of the magnetic microrobot according to its magnetic field. The algorithm developed to calculate the vector position is depicted in (Fig.8)

TABLE I

3D MAGNETIC SENSOR OUTPUT BEFORE AND AFTER THE CALIBRATION

	Positive direction		Negative direction	
	Before	After	Before	After
B_x	14,450568	4,25096	3,423852	-5,66775
B_y	5,2393277	-1,78097	9,5519505	1,84216
B_z	34,521553	22,3284	-12,451617	-20,1602

III. EXPERIMENTAL RESULTS

To validate the real-time localization proposed approach based on magnetic sensors, we have developed the experimental bench presented in (Fig.9). It composed of a micrometric positioning system (PI MicroMove) from Physik Instrument, two magnetic sensors GMR $(HMC1053)$ very sensitive $(1mv/v/Gauss)$, electronic part and localization interface. The positioning system can achieve a position accuracy of $< 1\ mum$. It is used to move the magnetic microrobot with micrometric precision. The electronic part consists of a power supply, an amplifier and an ADC acquisition of NI instruments and a three-dimensional magnetic sensor from Honeywell HMC-1053. The software part consists of the localization algorithm developed which is runs under Matlab and Labview.

A. Localization of a microrobot performing 2D motion

In the first experiment, we positioned the magnetic microrobot on the MicroMove system that we programmed to achieve a circular trajectory. The (Fig.10) shows the circular motion made by the 3D positioning system and the circular motion provided by the localization algorithm. As we can

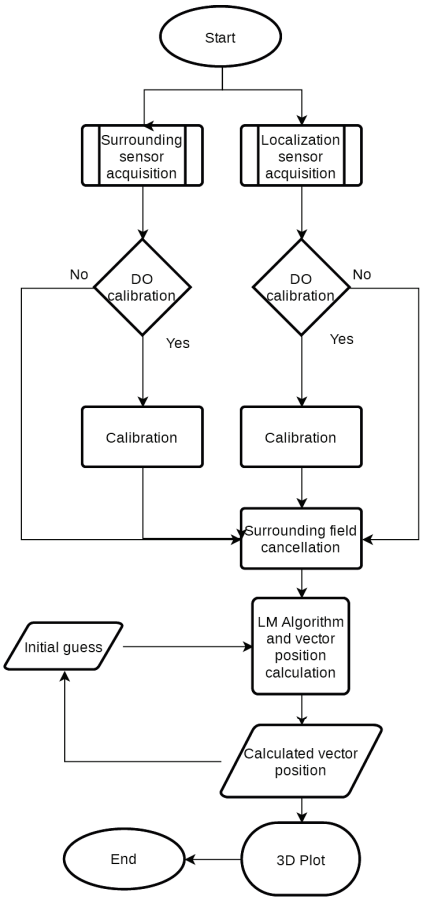

Fig. 8. Localization algorithm.

see the two circles are perfectly identical for the calibrated sensor but present more then 2mm errors for the uncalibrated sensor.

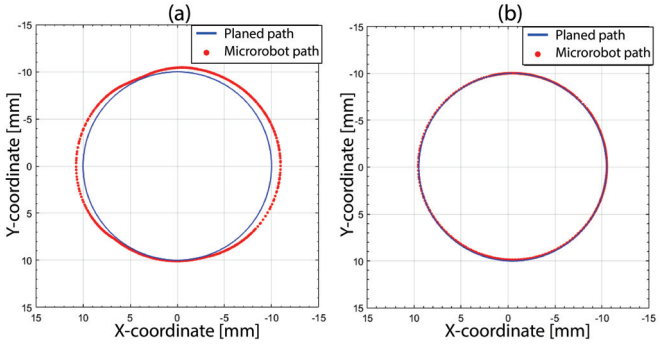

Fig. 10. Localization of the microrobot performing a 2D motion: (a) localization result without calibartion, (b) localization result with calibartion.

The second experiment demonstrates the possibility of localizing the magnetic microrobot in 3D motion. As in the previous experiment, the magnetic microrobot is positioned on the MicroMove system. Then it is programmed to achieve a 3D motion like cochlea canal (Fig.11). As we can see the movement of the magnetic microrobot recorded by the localization algorithm corresponds to the movement made by the MicroMove system.

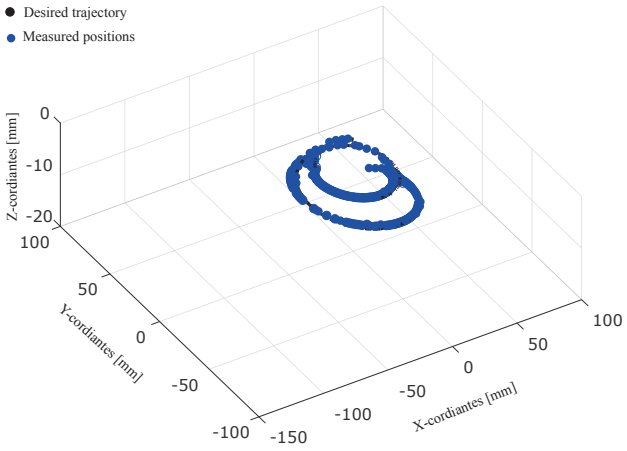

Fig. 11. Localization of the microrobot performing a 3D motion (Cochlea).

IV. CONCLUSIONS

A Real-time Localization System based on Magnetic Sensors for 3D magnetic microrobot Navigation has been proposed. To obtain high localization accuracy, a robust algorithm was developed and a novel calibration method for a magnetic sensor has been performed to obtain the compensation parameters. The comparison of the experimental results with theoretical analysis shows that our system is very competitive compared with existing similar techniques. The experimental results show that the system is more accurate after the calibration routine that decrease localization error to 0.1 mm of the position of the magnetic microrobot.

ACKNOWLEDGMENT

This work was supported by the CochleRob project, founded by HEI campus Centre, Châteauroux Métropole and Région Centre-Val de Loire, in France.

REFERENCES

[1] X. Gao, Y. Wang, K. Chen, B. P. Grady, K. J. Dormer, and R. D. Kopke, "Magnetic assisted transport of plga nanoparticles through a human round window membrane model," *Journal of Nanotechnology in Engineering and Medicine*, vol. 1, no. 3, p. 031010, 2010.

[2] S. Juhn, "Barrier systems in the inner ear," *Acta Oto-Laryngologica*, vol. 105, no. sup458, pp. 79–83, 1988.

[3] O. Sterkers, E. Ferrary, and C. Amiel, "Production of inner ear fluids." *Physiological reviews*, vol. 68, no. 4, pp. 1083–1128, 1988.

[4] C.-S. Han, J.-R. Park, S.-H. Boo, J.-M. Jo, K.-W. Park, W.-Y. Lee, J.-G. Ahn, M.-K. Kang, B.-G. Park, and H. Lee, "Clinical efficacy of initial intratympanic steroid treatment on sudden sensorineural hearing loss with diabetes," *Otolaryngology–Head and Neck Surgery*, vol. 141, no. 5, pp. 572–578, 2009.

[5] A. A. McCall, E. E. L. Swan, J. T. Borenstein, W. F. Sewell, S. G. Kujawa, and M. J. McKenna, "Drug delivery for treatment of inner ear disease: current state of knowledge," *Ear and hearing*, vol. 31, no. 2, p. 156, 2010.

[6] M. V. Goycoolea and L. Lundman, "Round window membrane. structure function and permeability: a review," *Microscopy research and technique*, vol. 36, no. 3, pp. 201–211, 1997.

[7] K. S. Alzamil and F. H. Linthicum Jr, "Extraneous round window membranes and plugs: possible effect on intratympanic therapy," *Annals of Otology, Rhinology & Laryngology*, vol. 109, no. 1, pp. 30–32, 2000.

[8] S. K. Plontke and A. N. Salt, "Local drug delivery to the inner ear: Principles, practice, and future challenges." *Hearing research*, vol. 368, pp. 1–2, 2018.

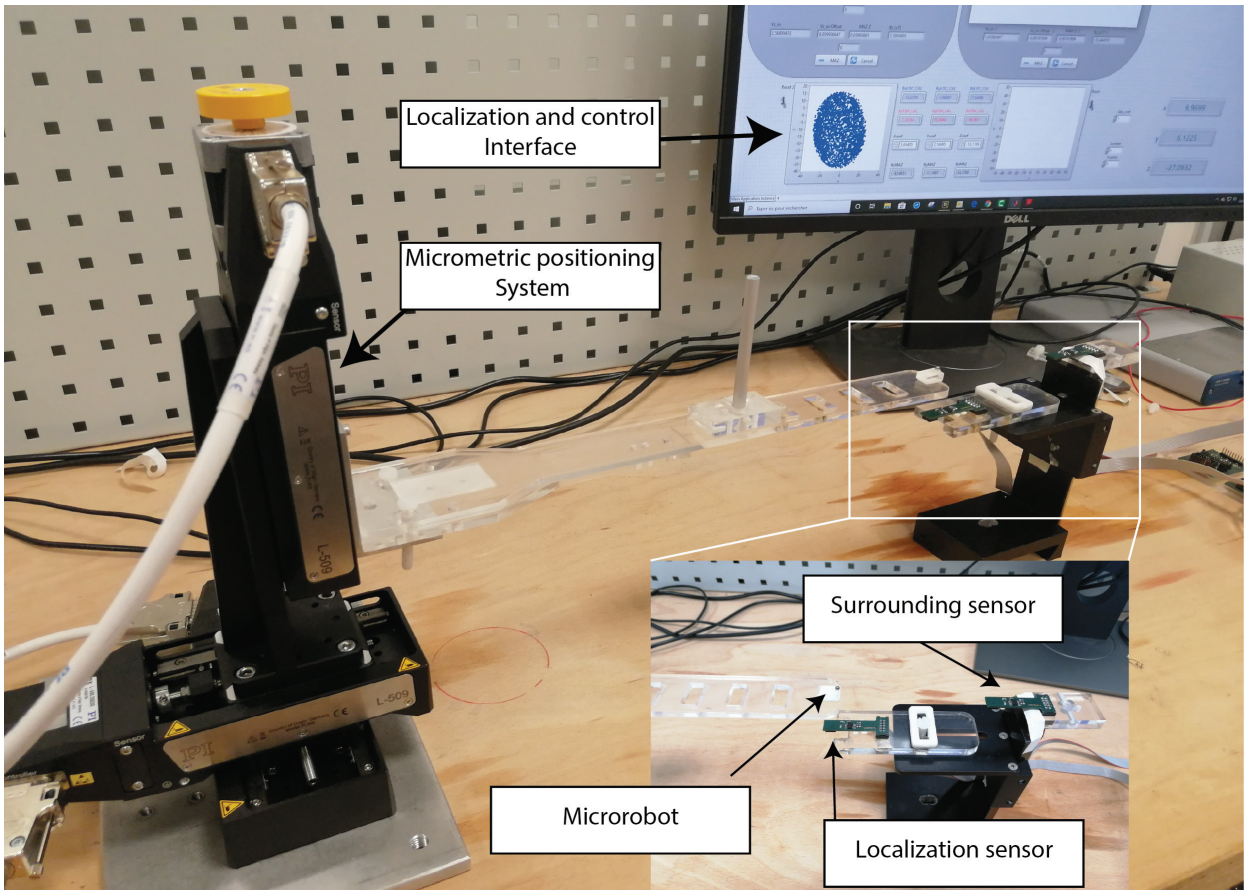

Fig. 9. Overall experimental system setup for microrobot localization.

[9] W. Amokrane, K. Belharet, M. Souissi, A. B. Grayeli, and A. Ferreira, "Design and prototyping of a magnetic actuator based permanent magnets for microbead navigation in viscous environment," in *2017 IEEE/RSJ International Conference on Intelligent Robots and Systems (IROS)*. IEEE, 2017, pp. 395–400.

[10] ——, "Macro–micromanipulation platform for inner ear drug delivery," *Robotics and Autonomous Systems*, vol. 107, pp. 10–19, 2018.

[11] M. Abbes, K. Belharet, H. Mekki, and G. Poisson, "Permanent magnets based actuator for microrobots navigation," in *2019 IEEE/RSJ International Conference on Intelligent Robots and Systems (IROS)*. IEEE, 2019, pp. 7062–7067.

[12] G. Leterme, C. Guigou, A. Oudot, B. Collin, J. Boudon, N. Millot, A. Geissler, K. Belharet, and A. Bozorg Grayeli, "Superparamagnetic nanoparticle delivery to the cochlea through round window by external magnetic field: Feasibility and toxicity," *Surgical innovation*, vol. 26, no. 6, pp. 646–655, 2019.

[13] S. Martel, "Microrobotics in the vascular network: present status and next challenges," *Journal of Micro-Bio Robotics*, vol. 8, no. 1, pp. 41–52, 2013.

[14] D. Son, X. Dong, and M. Sitti, "A simultaneous calibration method for magnetic robot localization and actuation systems," *IEEE Transactions on Robotics*, vol. 35, no. 2, pp. 343–352, 2018.

[15] Z. Sun, L. Maréchal, and S. Foong, "Passive magnetic-based localization for precise untethered medical instrument tracking," *Computer methods and programs in biomedicine*, vol. 156, pp. 151–161, 2018.

[16] I. S. Khalil, A. Adel, D. Mahdy, M. M. Micheal, M. Mansour, N. Hamdi, and S. Misra, "Magnetic localization and control of helical robots for clearing superficial blood clots," *APL bioengineering*, vol. 3, no. 2, p. 026104, 2019.

[17] G. Shao, Y. Tang, L. Tang, Q. Dai, and Y.-X. Guo, "A novel passive magnetic localization wearable system for wireless capsule endoscopy," *IEEE Sensors Journal*, vol. 19, no. 9, pp. 3462–3472, 2019.

[18] M. Wang, Q. Shi, S. Song, C. Hu, and M. Q.-H. Meng, "A novel relative position estimation method for capsule robot moving in gastrointestinal tract," *Sensors*, vol. 19, no. 12, p. 2746, 2019.

[19] C. Hu, M.-H. Meng, M. Mandal, and X. Wang, "3-axis magnetic sensor array system for tracking magnet's position and orientation," in *2006 6th World Congress on Intelligent Control and Automation*, vol. 2. IEEE, 2006, pp. 5304–5308.

[20] C. Hu, W. Yang, D. Chen, M. Q.-H. Meng, and H. Dai, "An improved magnetic localization and orientation algorithm for wireless capsule endoscope," in *2008 30th Annual International Conference of the IEEE Engineering in Medicine and Biology Society*. IEEE, 2008, pp. 2055–2058.

[21] V. Schlageter, P.-A. Besse, R. Popovic, and P. Kucera, "Tracking system with five degrees of freedom using a 2d-array of hall sensors and a permanent magnet," *Sensors and Actuators A: Physical*, vol. 92, no. 1-3, pp. 37–42, 2001.

[22] W. Andrä, H. Danan, W. Kirmße, H.-H. Kramer, P. Saupe, R. Schmieg, and M. E. Bellemann, "A novel method for real-time magnetic marker monitoring in the gastrointestinal tract." *Physics in medicine and biology*, vol. 45, no. 10, pp. 3081–3093, 2000.

[23] D. K. Cheng, *Field and Wave Electromagnetics*. Addison-Wesley, 1989.

[24] D. Gebre-Egziabher, G. H. Elkaim, J. David Powell, and B. W. Parkinson, "Calibration of strapdown magnetometers in magnetic field domain," *Journal of Aerospace Engineering*, vol. 19, no. 2, pp. 87–102, 2006.

[25] S. Su, W. Yang, H. Dai, X. Xia, M. Lin, B. Sun, and C. Hu, "Investigation of the relationship between tracking accuracy and tracking distance of a novel magnetic tracking system," *IEEE Sensors Journal*, vol. 17, no. 15, pp. 4928–4937, 2017.

[26] D. W. Marquardt, "An algorithm for least-squares estimation of nonlinear parameters," *Journal of the society for Industrial and Applied Mathematics*, vol. 11, no. 2, pp. 431–441, 1963.